

# Biogas to Syngas through the Combined Steam/Dry Reforming Process: An Environmental Impact Assessment

Nicola Schiaroli,\* Mirco Volanti,\* Antonio Crimaldi, Fabrizio Passarini, Angelo Vaccari, Giuseppe Fornasari, Sabrina Copelli, Federico Florit, and Carlo Lucarelli\*

Cite This: *Energy Fuels* 2021, 35, 4224–4236

Read Online

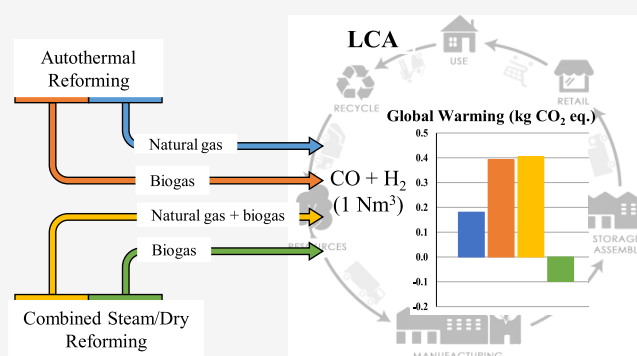
ACCESS |

Metrics & More

Article Recommendations

Supporting Information

**ABSTRACT:** The combined steam/dry reforming (S/DR) technology was used to produce syngas from clean biogas. In the reaction conditions proposed, the catalytic bed can produce, without deactivation, a syngas with a  $H_2/CO$  ratio of  $\approx 2$  directly processable for methanol or Fischer–Tropsch syntheses. Starting from the laboratory data obtained in the industrial conditions, mass and energy balances for the overall process were obtained from Aspen HYSYS simulations. The environmental evaluation was performed by applying the life cycle assessment (LCA) methodology, comparing different scenarios to the current industrial route to produce syngas (autothermal reforming or ATR of natural gas). The analysis showed that clean biogas-to-syngas technology using reforming processes has the potential to reduce the anthropogenic impact on the environment. The ReCiPe method showed that when the combined S/DR process is conducted using clean biogas also as a heat source, the  $CO_2$  balance turns negative, ensuring that the whole process has excellent potential as carbon capture and utilization (CCU) technology providing the lowest damage in all categories. Its improvement would make it possible to further reduce the environmental burden of the overall process, which is essential for achieving sustainable development.



possible to produce valuable products such as methanol and/or liquid fuels via Fischer–Tropsch synthesis. The latter are highly consolidated chemical industry processes, which in the last decades have been extensively reviewed and optimized in different operating conditions.<sup>7–9</sup> One of the most important requirements of these systems in terms of productivity and ease of operations (that consequently reduce their environmental impact) is to convert syngas with an optimal  $H_2/CO$  ratio ( $\sim 2$  v/v). This gaseous stream can be produced by different reforming technologies that are nowadays exploited to convert natural gas in centralized and high production plants.<sup>10</sup> These processes represent the most energy-intensive step of the production chain<sup>11</sup> and can consequently greatly influence the impact of the overall gas-to-liquid system on the environment.

The autothermal reforming (ATR) is a combined combustion and catalytic process that has been used to produce  $H_2$ - or  $CO$ -rich syngas from natural gas for decades.<sup>10,12</sup> The reaction takes place in an adiabatic reactor that consists of a burner, a

possible to produce valuable products such as methanol and/or liquid fuels via Fischer–Tropsch synthesis. The latter are highly consolidated chemical industry processes, which in the last decades have been extensively reviewed and optimized in different operating conditions.<sup>7–9</sup> One of the most important requirements of these systems in terms of productivity and ease of operations (that consequently reduce their environmental impact) is to convert syngas with an optimal  $H_2/CO$  ratio ( $\sim 2$  v/v). This gaseous stream can be produced by different reforming technologies that are nowadays exploited to convert natural gas in centralized and high production plants.<sup>10</sup> These processes represent the most energy-intensive step of the production chain<sup>11</sup> and can consequently greatly influence the impact of the overall gas-to-liquid system on the environment.

Received: December 2, 2020

Revised: February 7, 2021

Published: February 18, 2021



## 1. INTRODUCTION

Reinventing the energy and chemical market to overcome the intensive use of fossil fuels through the efficient exploitation of renewable sources is an essential step to reduce the anthropogenic impact on the environment. In this context, a better exploitation of biogas can deal with the increasing amount of organic wastes produced by modern societies and the reduction of greenhouse gas (GHG) emissions, providing a way to overtake two of the main modern life challenges and to integrate rural communities and industries into the transformation of the energy sector.<sup>1</sup> Delocalized small plants can in fact produce biogas by the anaerobic fermentation of biomasses and/or wastes through technologies such as biodigesters, landfill gas recovery systems, and wastewater treatment plants.<sup>2–4</sup> The composition of biogas depends on the type of feedstock processed and on the production pathway but, after its purification (to remove  $H_2S$ ,  $NH_3$ ,  $H_2O$ , and siloxanes), it is composed of only  $CH_4$  (45 up to 75%) and  $CO_2$  (clean biogas, CB).<sup>5</sup> Upon removing  $CO_2$ , biomethane (BM) is obtained that can be transported and used in the same way as natural gas, as it is indistinguishable from it.<sup>6</sup> On the other hand, BM production valorizes only half of the resources. A different but appealing application of CB lies in its valorization through gas-to-liquid systems. Through the production of synthesis gas (syngas, a mixture of  $H_2$  and  $CO$ ) as an intermediate step, it is indeed

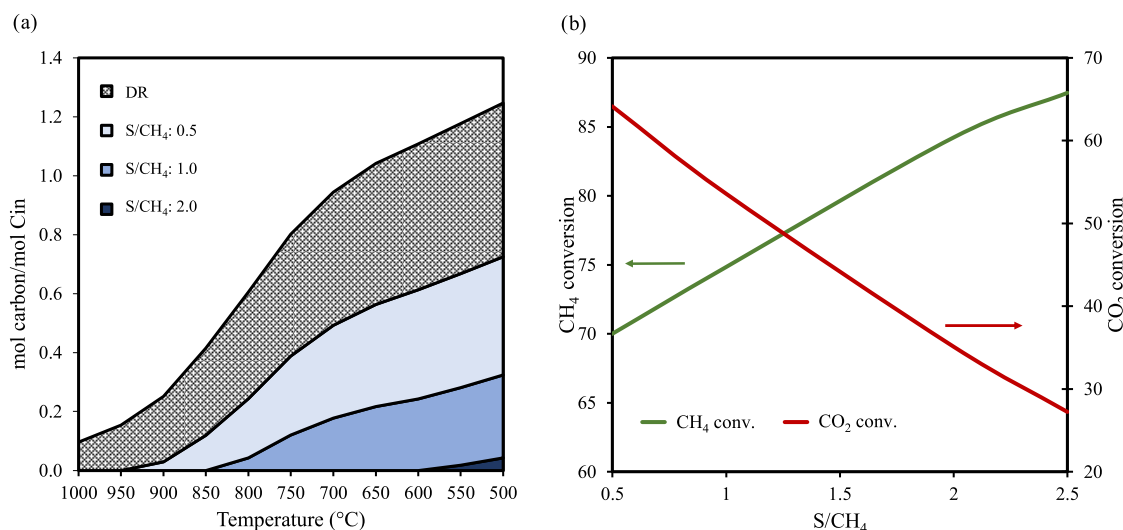


**Figure 1.** (a) Carbon formation curves expressed as mol of carbon formed/mol of carbon in the inlet stream ( $C_{in}$ ), at the thermodynamic equilibrium calculated at 30 bar with an equimolar mixture of  $CH_4$  and  $CO_2$  in the inlet stream, as a function of temperature and S/ $CH_4$  ratio (DR conditions, S/ $CH_4$  = 0.0). (b) Conversion of  $CH_4$  and  $CO_2$  at the thermodynamic equilibrium as a function of S/ $CH_4$  ratio in the inlet stream at 900 °C and 30 bar.

combustion chamber, and a fixed-bed catalyst, contained in a refractory lined pressure shell. A mixture of methane, oxygen, and steam (S) is partially converted in a pressurized combustion chamber. A CO-rich syngas can be produced as a feedstock for methanol synthesis, most conveniently synthesized using syngas with low steam content, as demonstrated at the pilot and industrial scale.<sup>13</sup> The temperature of the process is around 1100–1300 °C near the catalyst bed, reaching 2500 °C in the flame core. This zone can be characterized by a single reaction of  $CH_4$  to CO and  $H_2O$  with an  $O_2/CH_4$  ratio of the chosen stoichiometry, while in the catalytic zone, the final conversion through the heterogenous reaction of hydrocarbons takes place (eqs 1 and 2) to produce syngas with different  $H_2/CO$  ratios, depending on the operating conditions.<sup>10</sup>

steam reforming (SR):  $CH_4 + H_2O \rightleftharpoons CO + 3H_2$ ;

$$\Delta H_{298K} = +206 \text{ kJ/mol} \quad (1)$$

water gas shift (WGS):  $CO + H_2O \rightleftharpoons CO_2 + H_2$ ;

$$\Delta H_{298K} = -41 \text{ kJ/mol} \quad (2)$$

This technology is also used by H. Topsøe A/S in the two-step reforming of natural gas or in a stand-alone reactor to subsequently produce methanol.<sup>14</sup> The SR of  $CH_4$  is the most common and cost-effective method for syngas production. The reaction is highly endothermic, and it is typically carried out at 20–40 bar and at 800–1000 °C using a Ni-based catalyst placed in multiple fixed-bed tubular reactors contained in a heated furnace. A generator produces high-temperature steam that is sent to the reformer after being mixed with the carbonaceous gas stream. The heat required for the reaction is provided by the burning part of the natural gas fed.<sup>15–17</sup> This combustion produces an exhaust stream that can be thermally valorized through different heat exchangers placed before the reforming reactor. One of the main drawbacks of this process is that a syngas suitable for a gas-to-liquid system is hardly attainable through a one-step steam reforming reactor (eq 1) that, due to the excess of steam used in the process, can easily promote the occurrence of the water gas shift (WGS) reaction (eq 2) producing syngas with  $H_2/CO > 3$ . It is noteworthy that the

appropriate syngas composition could be obtained from biogas through the valorization of its  $CO_2$  content.<sup>18–21</sup> As also demonstrated in our previous work,<sup>22</sup> CB can be effectively converted to syngas in a combined reforming process that couples the SR (eq 1) and the dry reforming (DR) reaction (eq 3) in one reactor.

dry reforming (DR):  $CH_4 + CO_2 \rightleftharpoons 2CO + 2H_2$ ;

$$\Delta H_{298K} = +247 \text{ kJ/mol} \quad (3)$$

The DR reaction converts the  $CO_2$  to a CO-rich syngas but has many drawbacks related to the high endothermicity and high C-formation rate that limits the catalyst durability and the safety of the plant.<sup>15,23,24</sup> From the C-formation curves calculated at the thermodynamic equilibrium (Figure 1a), it is possible to observe that, working in pure DR conditions, the C formation is favored in all range of reaction temperatures, becoming low only at  $T > 1000$  °C (30 bar). When steam is added to the inlet stream to perform the combined steam/dry reforming (S/DR) reaction, C formation decreases and becomes negligible for S/ $CH_4 > 2$  regardless of reaction conditions considered.

This combined process produces a syngas with a  $H_2/CO$  ratio that varies as a function of the amount of steam fed. The quantity of water drives the global reaction favoring one reaction over the other and, consequently, increasing the  $CO_2$  conversion when the amount of steam is low, and the DR is favored (Figure 1b).

In the present work, the use of a sustainable combined S/DR technology to obtain syngas from CB is proposed. Life cycle assessment (LCA) is a well-established methodology to assess the potential environmental impacts and resources used throughout the entire life cycle of a process or product. Using this tool, Hakawati et al.<sup>25</sup> evaluated the efficiency of different biogas utilization routes finding that although the direct use of biogas (to produce energy) has the best efficiency, this path limits its use to sites collocated with the anaerobic digestion facility, hindering its wider exploitation. Hajjaji et al.<sup>26</sup> evaluated the environmental impact of the biogas reforming to produce hydrogen, finding that although the anaerobic digestion process negatively affects the LCA results, a potential abatement of about half of the life cycle GHG of conventional  $H_2$  production systems can be achieved. In this context, Battista et al.<sup>27</sup>

proposed a process to produce  $H_2$  from biogas through ATR, reducing emissions and lowering the energetic impacts, while Di Marcoberardino et al.<sup>28</sup> showed that the adoption of a Pd membrane reactor that allows the simultaneous  $H_2$  production and separation increases the system efficiency, lowering the impacts and thus promoting the substitution of more hydrogen produced by fossil fuels. The environmental assessment of biogas valorization via the DR reaction and Fischer–Tropsch synthesis to produce fuels was carried out by Navas-Anguila et al.,<sup>29</sup> where through the simulation of the process it was found that the production of synthetic biodiesel was not environmentally favorable. In this sense, further optimization of the biogas-to-liquid system would be needed as the major contributors to undesired emissions were the biogas production, methane leakage, and the high heat demand of the system. The combination of DR and partial oxidation (in two different reactors) to produce syngas suitable for methanol synthesis can effectively decrease the environmental impact of the process,<sup>30</sup> but the drawbacks related to the use of a DR reactor can limit its scalability. Chen et al.<sup>31</sup> evaluated the sustainability of a combined S/DR process for syngas production, comparing the results with a tri-reforming process (a combination of SR, DR, and partial oxidation). The use of two distinct reforming reactors (one for the SR and the other for the DR) allowed adjusting the  $H_2/CO$  of the outlet stream by the blending of the produced syngas stream but limited the sustainability of the plant. On the other hand, using a single tri-reforming reactor, its sustainability through better energy savings and flue gas utilization was assured. A mixed reforming of NG,  $CO_2$ , and  $H_2O$  to produce syngas for methanol synthesis was also investigated by Shi et al.<sup>11</sup> By feeding a small amount of  $CO_2$  to the SR reactor ( $CO_2/CH_4 = 0.29$  v/v), the authors found that using the combined reforming, the methanol productivity increased but, because of the choice to use the purge gas stream as the main source of fuel for the reformer furnace, no improvements in terms of  $CO_2$  emissions were achieved. Proceeding from these premises, the study aimed to investigate the industrial conditions needed to decrease the environmental impact of the S/DR process. A single-reactor configuration is proposed, and the investigation of the process potential as carbon capture and utilization (CCU) technology was carried out by optimizing the different operative conditions and critically analyzing the heating system as well as the fuel used to heat the reactor. The feasibility of the process was at first assessed in a semipilot plant and then scaled-up through different Aspen HYSYS simulations of an industrial reforming reactor. The investigation of different scenarios was carried out, and the environmental performances were evaluated and compared with the current syngas production technology.

## 2. EXPERIMENTAL SECTION

**2.1. Lab-Scale Data.** To obtain representative data for the S/DR process, the reaction was first performed in a semipilot plant. The aim was to validate the feasibility of the process using an industrial-like catalyst and thus creating an experimental basis for the process simulation and its LCA evaluation. The reaction was conducted using a Ni/Rh-based catalyst optimized in our previous work<sup>22</sup> and obtained by the coprecipitation of a hydrotalcite-type (HT) precursor followed by calcination at 900 °C for 6 h. The obtained mixed/oxide catalyst after reduction has the composition reported in Table 1.

The pelletized catalyst (particle diameter between 0.420 and 0.595 mm) was loaded in a tubular reactor (INCOLOY 800HT, i.d. = 8 mm) between the two layers of quartz and vertically placed into an electrical tubular furnace. The feasibility of the S/DR reaction was tested feeding

**Table 1. Catalyst Composition Expressed as Percentages by Weight of the Different Metals after the Reduction Step**

catalyst	Ni (wt %)	Rh (wt %)	Mg (wt %)	Al (wt %)
Ni–Rh/Mg/Al/O	10.0	0.5	38.8	12.0

an equimolar mixture of  $CH_4$  and  $CO_2$  with S/ $CH_4$  equal to 2. The tests were carried out at a pressure of 5 bar (to simulate the pressure effects that occur in the industrial plants) and a reaction temperature of 900 °C maintaining a constant gas hourly space velocity (GHSV) of 50 000 mL/(h·g<sub>cat</sub>). Before the reaction, the in situ reduction of the catalyst was carried out feeding a continuous flow of  $H_2/N_2$  (1/10 v/v) at 5 bar increasing the catalyst temperature from 300 to 900 °C (10 °C/min) and holding this temperature for 1 h. The composition of the outlet stream was analyzed by an online gas chromatograph (Agilent Technology 7890A) equipped with a CarboPLOT (carrier gas  $H_2$ , for the detection of  $CO$ ,  $CO_2$ , and  $CH_4$ ) and an HP-Molesieve (carrier gas  $N_2$ , to quantify  $H_2$ ) columns and two thermal conductivity detectors (TCD).

The calculations of the thermodynamic equilibrium at different operating pressure and temperature were performed using CEAgui software distributed by NASA.<sup>32</sup>

**2.2. LCA Methodology.** To evaluate the environmental performances of the processes, the life cycle assessment (LCA) methodology was applied. It was carried out in agreement with ISO 14040:2006<sup>33</sup> and ISO 14044:2018,<sup>34</sup> which set out the guidelines and application methods. LCA methodology, as specified in the standards, consisted of four steps: (i) goal and scope definition, (ii) life cycle inventory (LCI), (iii) life cycle impact assessment, and (iv) interpretation. Nowadays, the LCA has an important literature on the impact assessment of industrial chemical processes<sup>35–41</sup> and its features are also used for early stage (AES) evaluations.<sup>42–45</sup> This approach consists of a preliminary analysis of the environmental impacts of the processes before they are developed at industrial level evaluations.<sup>36</sup> As for the economic aspect, this procedure saves time, energy, and money in developing alternatives that turn out to be environmentally worse than existing solutions.

The purpose of the study was to analyze, from a life cycle point of view, the environmental burden of the proposed combined S/DR reaction for syngas production compared to the current existing ATR process. Two scenarios for each technology were applied: the ATR was studied with natural gas (scenario A) or CB (scenario B) as raw materials, while both the S/DR scenarios used CB as a reagent, but in one case, the heating was supported by natural gas (scenario C) and in the other by CB (scenario D). The production of 1 N m<sup>3</sup> of syngas was set as a functional unit (FU) with which all of the scenarios were compared. The obtained syngas must have the same characteristics, i.e., a  $H_2/CO$  ratio of 1.95 and a purity higher than 92%. The FU ensures an unambiguous and standardized comparison between the scenarios, as required by the LCA methodology guidelines.

The system boundaries of the LCA extend from the production (or extraction) of the raw materials to the obtaining of the product (syngas), following an approach called “from-cradle-to-gate” analysis. The boundary was placed at the industrial gate because the fate of the syngas was not part of the scope of this environmental analysis. Figure 2 depicts the four scenarios and the system boundaries considered, showing the necessary processes for each pathway to obtain the same FU.

Scenarios were created using SimaPro software v.9.1<sup>46</sup> and its libraries; in particular, Ecoinvent database v3.5<sup>47</sup> was set as a reference database for all of the background information. The production of biogas was simulated with primary data from our previous work,<sup>48</sup> in which it was obtained from the anaerobic digestion of the organic fraction of municipal solid waste. Organic waste was considered impact-free, while all subsequent steps (including its processing and purification) were within the system boundaries. The impacts related to the extraction and use of natural gas were simulated with the process in the Ecoinvent 3.5 database “Natural gas, high pressure {GLO} market group for | Cut-off, U”.<sup>39</sup> In all scenarios, the demand for electricity was satisfied by the grid, while thermal consumption was

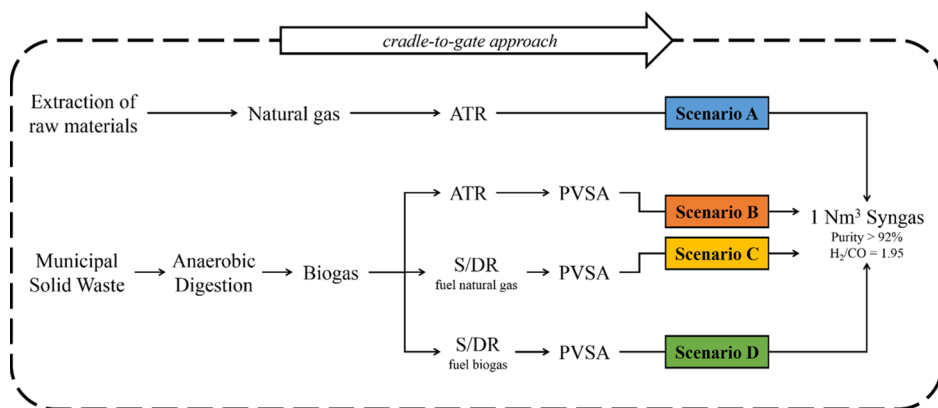


**Figure 2.** System boundaries and functional unit applied in this study (ATR = autothermal reforming, S/DR = steam/dry reforming, PVSA = pressure vacuum swing adsorption).

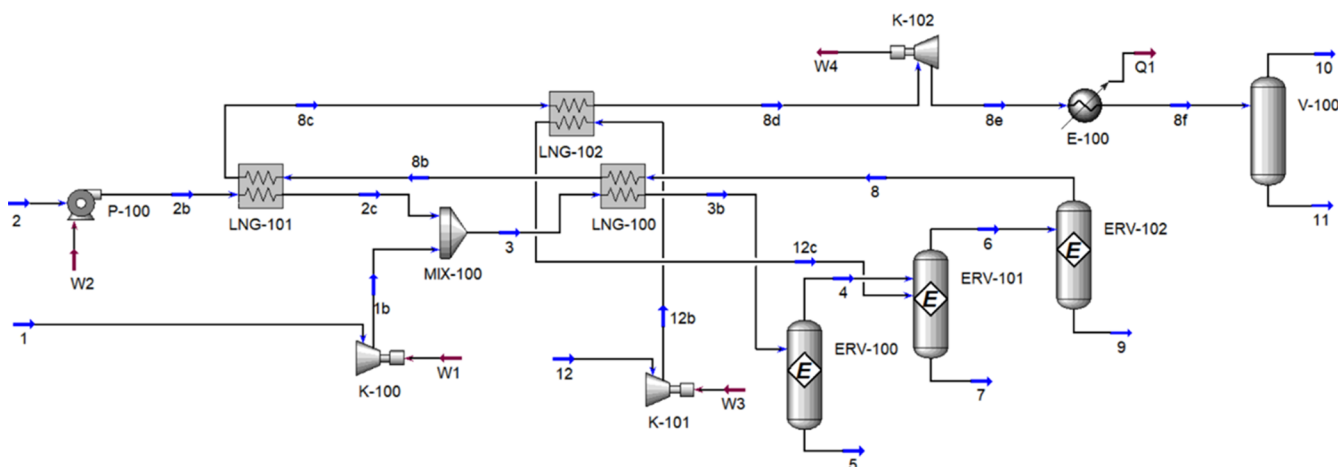


**Figure 3.** Process flow diagram (PFD) for the ATR of pure methane.

covered by the different gas sources (natural gas or CB). After the reactors, the models assumed that excess heat and electricity were recovered with a conversion efficiency of 50 and 31%, respectively.<sup>49</sup> With a zero-waste perspective and with the possibility of combining biogas upgrading plants with anaerobic digestion systems or with plants for the utilization of the syngas, these energy recoveries were considered as avoided impacts. Since it was not necessary to produce the same amount of thermal energy and electricity, directly or indirectly, from fossil fuels, this turned out to be an advantage for the environment. The environmental impacts of the four scenarios considered were evaluated using two methods of analysis that have already shown a proven synergy in these types of studies:<sup>37,50</sup> ReCiPe 2016<sup>51</sup> and cumulative energy demand (CED).<sup>52</sup> The first is a method to predict the environmental loads of a process/product through the assessment of burdens in several impact categories (such as global warming (GW), water consumption (WC), etc.). It is also able to translate the impacts (midpoint results) into damage caused to three receptors: human health, ecosystem quality, and resource consumption (endpoint level). On the other hand, the CED method analyzes the need for direct and indirect resources of a process, expressing the results in terms of energy equivalents (MJ equiv). It is a midpoint characterization method in which the resources are divided into renewable and nonrenewable categories.

**2.3. Process Description.** The feed considered was a model CB composed of an equimolar mixture of  $\text{CH}_4$  and  $\text{CO}_2$  that, after being mixed with hot steam, was sent to the reformer to be converted to syngas. To evaluate the advantages of the biogas-to-syngas technology, the current ATR technology for syngas production was also considered, where the feed was a pure  $\text{CH}_4$  stream. After the reaction, the reformer effluents were sent to a series of energy recovery steps and then, after decompression, to a condensing unit aimed at separating water from the

desired syngas. The dry gas further underwent a pressure vacuum swing adsorption (PVSA) to remove the unconverted  $\text{CO}_2$  and obtain a syngas with a purity (defined by the sum of the molar fractions of  $\text{H}_2$  and  $\text{CO}$ ) greater than 92%. The different technologies/schemes differed in the type of reactor used but produced the same quantity of syngas with the same purity, suitable for downstream applications such as Fischer–Tropsch or methanol synthesis.

In the following, such processes were simulated using Aspen HYSYS v7.3 software. In all schemes, the thermodynamic model used a Peng–Robinson equation of state to describe the behavior of the gaseous streams and possible vapor–liquid equilibria. All reactors were therefore considered as equilibrium reactors, although, in most cases, there was no liquid stream exiting the reactor.

**2.3.1. Scenario A: ATR of Natural Gas.** In the ATR process using pure methane (Figure 3),  $\text{CH}_4$  (stream 1, at room temperature and pressure) was compressed to 24.5 bar (K-100) and then mixed adiabatically (MIX-100) with a stream (2c) of hot steam (at the same pressure), coming from the second energy recovery step (LNG-101) of the stream (8) exiting from the second stage of the ATR reactor (ERV-101). Such a mixed stream (3) was then heated in the first energy recovery step (LNG-100) of stream 8 and then collected to a prereforming unit (ERV-100) where the SR and WGS reactions (eqs 1 and 2) took place (experimental equilibrium data were used to calculate the conversion at the reactor outlet).

The stream (4) exiting from ERV-100 was then sent to the first stage of the ATR process where the combustion with pure oxygen (initially compressed at 24.5 bar), and then further heated to 580 °C using the third energy recovery step of 8 (LNG-102) took place through the partial combustion reaction (eq 4)

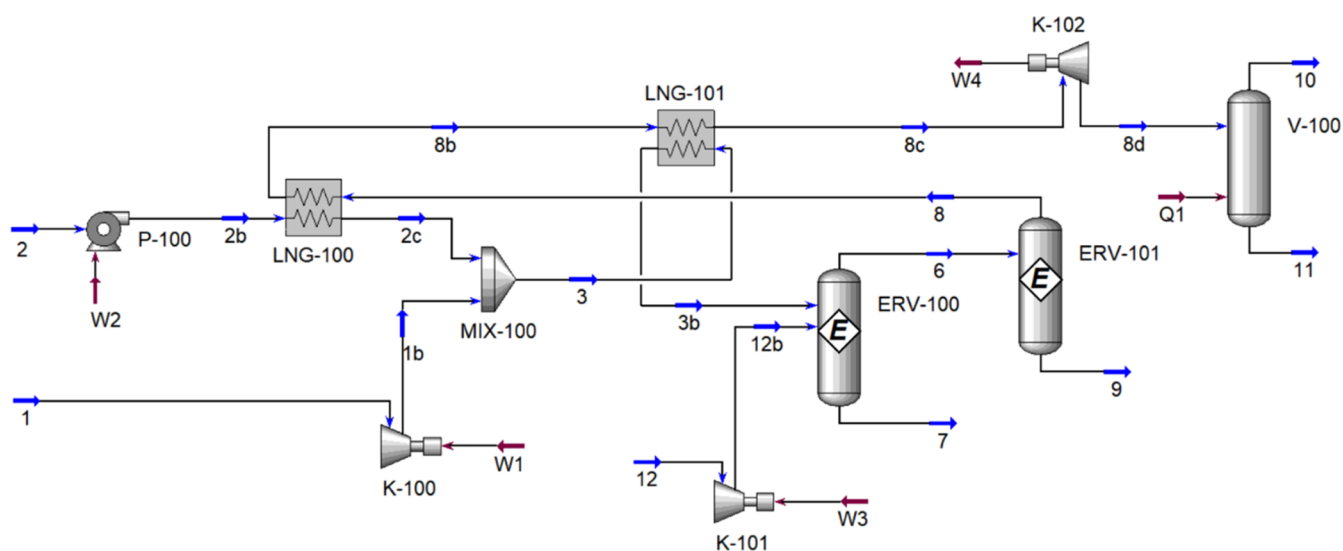


Figure 4. PFD for the ATR of biogas.

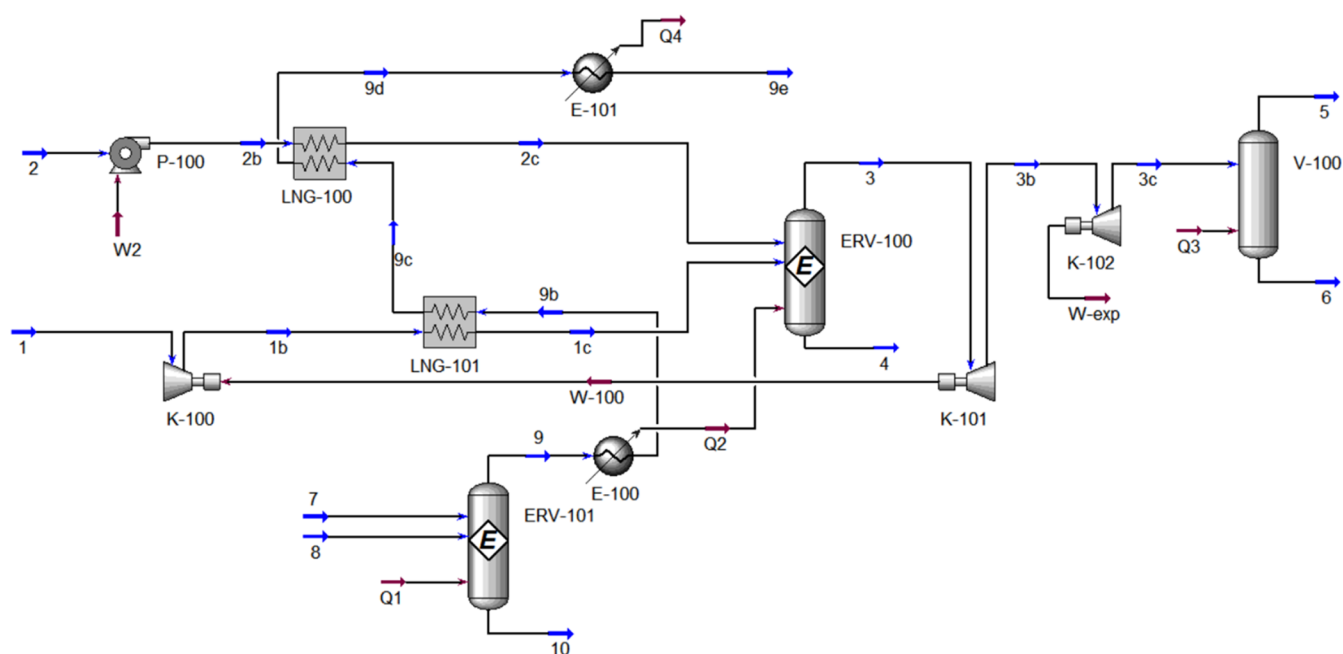
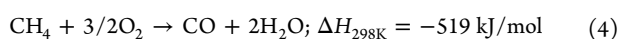


Figure 5. PFD for combined S/DR of biogas using pure methane as a heating supplier.



which was treated as an equilibrium reaction using a standard correlation of the Gibbs free energy to calculate the equilibrium constant ( $k_{\text{equiv}}$ ).

After this first stage of the ATR process, the hot stream (6) passed through a second stage where the SR and WGS reactions took place. The resulting stream (8) was then sent to the series of three energy recovery steps previously described and, finally, collected (8d) to an expander (K-102) and cooled (8e to 8f) to separate the water (11) from the gaseous stream (10).

**2.3.2. Scenario B: ATR of Clean Biogas.** In the ATR process using CB (Figure 4) as a raw material, the CB (stream 1, composition 50/50 (v/v)  $\text{CH}_4/\text{CO}_2$ , at room temperature and pressure) was compressed to 24.5 bar (K-100) and then mixed adiabatically (MIX-100) with a stream (2c) of hot steam at the same pressure coming from the first energy recovery step (LNG-100) of the stream 8 exiting from the second stage of the ATR reactor (ERV-101). Such a mixed stream (3) was then heated in the second energy recovery step (LNG-101) of

stream 8 and then directly collected to the first stage of the ATR process (ERV-100), where the combustion reaction with pure oxygen (compressed at 24.5 bar reaching 559 °C) took place. As discussed above, it was a partial combustion that was treated as an equilibrium reaction (a standard correlation of the Gibbs free energy was used to calculate  $k_{\text{equiv}}$ ).

After this first stage of the ATR process, the hot stream (6) passed through a second stage where the SR and WGS reactions took place. The resulting stream 8 was then sent to the series of two energy recovery steps previously described and, finally, collected (8c) to an expander (K-102) and cooled directly into the separator V-100 to separate the water (11) from the gaseous stream (10).

**2.3.3. Scenario C: S/DR of Clean Biogas: NG as a Fuel.** In the combined S/DR process of biogas using pure methane as a source for heating (Figure 5),  $\text{CH}_4$  (stream 8, at room temperature and pressure) was sent to an adiabatic equilibrium reactor (ERV-101) where the total combustion of methane with air (stoichiometric oxygen) took place. Such a unit simulates an ideal furnace with no heat losses; such a choice can be justified within the purpose of this work, which is to obtain

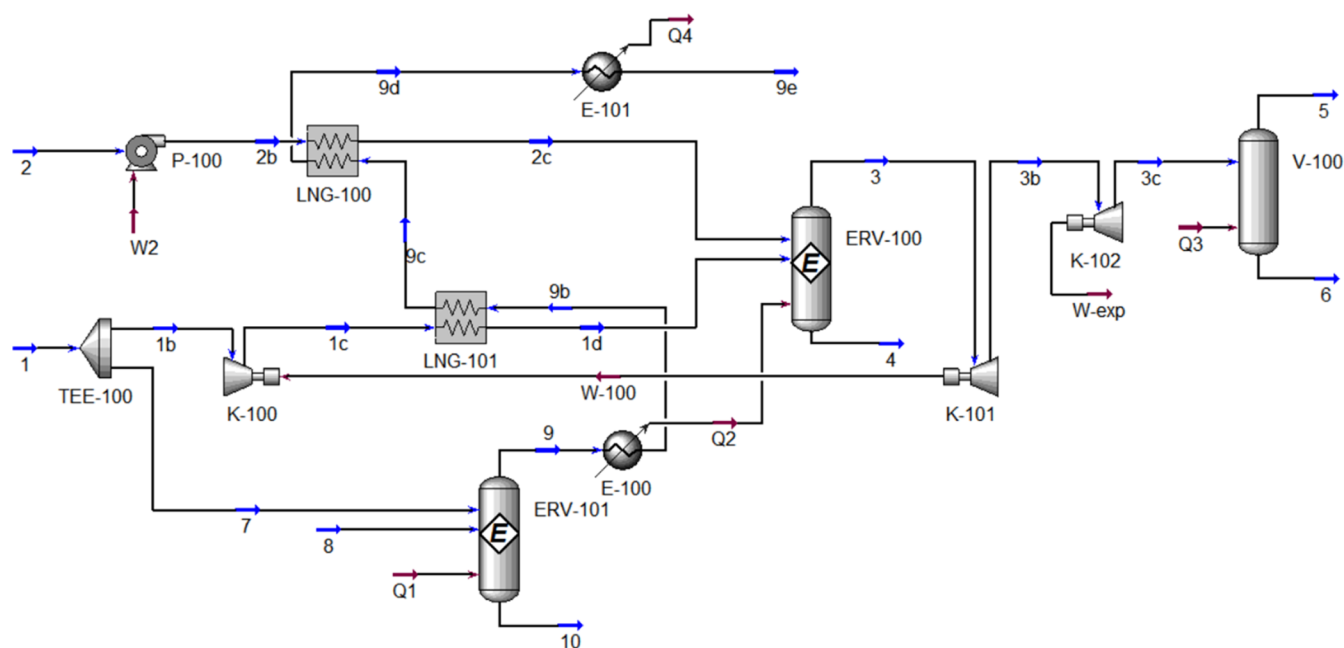


Figure 6. PFD for the combined S/DR of biogas using a fraction of it as a heating supplier.

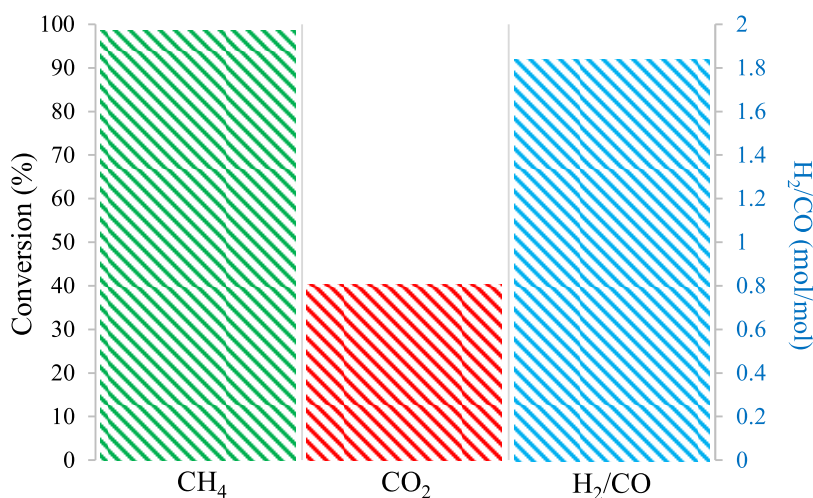


Figure 7. CH<sub>4</sub>, CO<sub>2</sub> conversion, and the H<sub>2</sub>/CO ratio observed at 900 °C, 5 bar, S/CH<sub>4</sub> = 2 using the Ni–Rh/Mg/Al/O catalyst.

reliable (even if approximated) values of both temperature and composition of the off-gasses being involved in all of the heat recovery steps of the process (a detailed dynamical simulation of the process itself is not required). The off-gasses coming from this process unit (9) were then used to heat the S/DR reactor (ERV-100) to 950 °C (with a thermal flux Q<sub>2</sub>) and then sent to a series of two-step energy recovery processes (that will be described in the following).

Biogas (stream 1, at room temperature and pressure) was compressed to 30 bar (K-100) and then heated to 750 °C in the first energy recovery step (LNG-101) of stream 9b. Liquid water (stream 2, at room temperature and pressure) was compressed to 30 bar using a pump (P-100) and then heated to 950 °C using the second step of the energy recovery process of 9c (LNG-100). Finally, streams 1c and 2c were collected to a S/DR unit (ERV-100) where the reactions from eqs 1 and 3 took place (experimental equilibrium data were used to calculate the conversion at the reactor outlet).

The stream exiting from ERV-100 (3) was then sent to the first stage expander (K-101), which was coupled with the compressor K-100 for a full recovery of mechanical energy, and then to a second stage expander K-102 that decreased the stream pressure to the room pressure. Finally,

the resulting stream was collected to a separating-cooling unit (V-100) to separate water (6) from the gaseous stream (5).

**2.3.4. Scenario D: S/DR of Clean Biogas: CB as a Fuel.** In the combined S/DR process of biogas using a fraction of it as a source for heating (Figure 6), biogas (stream 1, at room temperature and pressure) was split into two streams: the first one (7) was sent to the adiabatic equilibrium reactor (ERV-101) for the combustion (see the comments, above for the assumptions related to this unit) while the other (1b) was compressed to 30 bar (K-100) and then heated to 750 °C before being collected to the S/DR reactor (ERV-100). All of the other steps are the same as those previously described for the S/DR process heated by pure methane.

For more details and information about the different simulation results, the extended PFD with the relative material streams and compositions are available in the Supporting Information.

### 3. RESULTS AND DISCUSSION

**3.1. Lab-Scale Data.** To fully understand the catalyst behavior in real operating conditions, the catalytic data were first extrapolated using the semipilot plant. A catalytic test at 900 °C,

5 bar and with a GHSV of 50 000 mL/(h·g<sub>cat</sub>) was carried out. The results in terms of CH<sub>4</sub>, CO<sub>2</sub> conversion, and value of the H<sub>2</sub>/CO ratio of the outlet stream are shown in Figure 7.

In these conditions, the CB conversion value reached the thermodynamic equilibrium. The operating conditions were appropriately studied to obtain a representative test by which the following scale-up could be considered reasonably adherent to the truth. The thermodynamics forces the decrease of the equilibrium conversions when the operating pressure is increased, leading to a lower product yield. Nevertheless, industrial reforming is usually conducted at ~30 bar. Since the reaction occurs in the gas phase, the increase in pressure allows processing an amount of reactant per unit of volume proportionally larger. The resulting increase of productivity covers the loss in conversion. The choice to work at 5 bar was, in this case, made for the following reasons: (i) the use of a lower amount of reactants for performing the test; (ii) the equilibrium conversion achievement with this catalyst allows extending the results for any range of pressure forcing the realization of equilibrium. The combined S/DR converted almost all of the CH<sub>4</sub> and a notable fraction of the CO<sub>2</sub> fed (≈40% v/v), producing syngas with a H<sub>2</sub>/CO molar ratio of 1.85. The lab-scale data demonstrated the feasibility of the combined S/DR and the possibility to valorize a CO<sub>2</sub>-rich CB in the presence of steam. Therefore, a simulation considering an industrial-scale operating conditions was carried out. To do this, the conditions were modulated considering an operative pressure of 30 bar and a temperature of 950 °C, adjusting the S/CH<sub>4</sub> value to obtain an outlet stream with a similar unconverted CO<sub>2</sub> content (Table 2).

**Table 2. Composition of the Outlet Stream of the S/DR of CB<sup>a</sup>**

conditions	CH <sub>4</sub> (mol %)	CO <sub>2</sub> (mol %)	CO (mol %)	H <sub>2</sub> (mol %)	H <sub>2</sub> O (mol %)
1	0.1	10.0	23.3	43.0	23.6
2	1.0	10.4	20.0	38.9	29.7

<sup>a</sup>Condition 1:  $T = 900$  °C,  $P = 5$  bar,  $S/CH_4 = 2.0$  mol/mol. Condition 2:  $T = 950$  °C,  $P = 30$  bar,  $S/CH_4 = 2.5$  mol/mol.

In particular, we made the assumption that the equilibrium has to be reached and the ratio between H<sub>2</sub> and CO must be almost constant. By increasing the S/CH<sub>4</sub> value to 2.5, it was possible to obtain a syngas with a H<sub>2</sub>/CO ratio of 1.95 suitable for methanol synthesis without drastically decreasing the CB conversion value (CH<sub>4</sub> conversion = 94%, CO<sub>2</sub> conversion = 33%; calculated at the thermodynamic equilibrium).

**3.2. Simulation Results: Mass and Energy Balance.** The raw results obtained from the ATR and combined S/DR processes are presented in Table 3. The differences in the order of magnitude of the different extrapolated values reflect the two distinct sources of data used for the simulations. While the balances of scenarios C and D were calculated starting from the experimental lab-scale data, the results for the two ATR scenarios (A and B) were simulated, starting from literature data,<sup>11,14</sup> through Aspen HYSYS v7.3 to obtain comparable results in both terms of similar H<sub>2</sub>/CO ratio value in the outlet stream as well as similar CH<sub>4</sub> inlet flow (the main source of CO in the process).

Although the ATR reactor is a self-sustained vessel from a thermal point of view (neutral thermal energy balance of scenarios A and B), the heat generated by burning natural gas (scenario C) or CB (scenario D) produced a huge amount of energy that can be partially utilized in different heat recovery systems of the plant, leading to a surplus of not-exploited energy in the case of both scenarios C and D. From the conversion values obtained, it was possible to observe that the use of an ATR technology led to higher CH<sub>4</sub> conversion values, e.g., almost the total fraction of natural gas was converted into the scenario A. On the other hand, the copresence of O<sub>2</sub> and H<sub>2</sub>O in the ATR inlet stream suppressed the CO<sub>2</sub> conversion (scenario B), hardly exploitable in reaction conditions, in which SR (eq 1) and partial combustion (eq 4) were most favored. As a result, CO<sub>2</sub> was produced through the WGS reaction (eq 2) in the prereformer (ERV-100 in Figure 2) used for the scenario A and from CH<sub>4</sub> total combustion and WGS in the ATR reactor of scenarios A and B. Although the CH<sub>4</sub> conversion values attained in scenarios C and D were lower (but still at 94% v/v), one-third of the CO<sub>2</sub> fed was valorized to obtain CO by DR (eq 3).

**Table 3. Raw Mass and Energy Balances of the Considered Scenarios<sup>a</sup>**

		scenario A	scenario B	scenario C	scenario D	unit
input	natural gas (CH <sub>4</sub> )	3600 <sup>c</sup>		$0.650 \times 10^{-6}$ <sup>b</sup>		kg mol/h
	biogas (CH <sub>4</sub> /CO <sub>2</sub> = 1)		6344 <sup>c</sup>	$1.269 \times 10^{-6}$ <sup>c</sup>	$1.269 \times 10^{-6}$ <sup>c</sup> $1.531 \times 10^{-6}$ <sup>b</sup>	kg mol/h
	water	450	3068	$1.586 \times 10^{-6}$	$1.586 \times 10^{-6}$	kg mol/h
	oxygen	2124	7930			kg mol/h
	air			$6.200 \times 10^{-6}$	$7.300 \times 10^{-6}$	kg mol/h
output	dry outlet stream	10 690	12 340	$2.971 \times 10^{-6}$	$2.971 \times 10^{-6}$	kg mol/h
	water condensed	493	8140	$1.077 \times 10^{-6}$	$1.077 \times 10^{-6}$	kg mol/h
	CO <sub>2</sub> (produced)	35.28	300	$0.65 \times 10^{-6}$	$0.77 \times 10^{-6}$	kg mol/h
	CO <sub>2</sub> (converted)		-9.46	33.65	33.65	% v/v
	CH <sub>4</sub> (converted)	99.02	97.86	94.01	94.01	% v/v
	H <sub>2</sub> /CO	1.97	1.96	1.94	1.94	v/v
energy	produced (thermal)			+0.5713	+0.6719	kJ/h
	heat Recovery			-0.3125	-0.3125	kJ/h
	compressors	$-1.153 \times 10^8$	$-2.765 \times 10^7$	-0.0551	-0.0551	kJ/h
	condenser	$-1.850 \times 10^8$	$-3.493 \times 10^8$	-0.1023	-0.1023	kJ/h
	total	$-2.338 \times 10^8$	$-3.770 \times 10^8$	+0.1014	+0.2020	kJ/h

<sup>a</sup>The results are expressed in terms of input and output flows, reactant conversions, and energy demand. The sign “-” represents a required energy while the “+” the energy produced. <sup>b</sup>Used as a fuel. <sup>c</sup>Used as a reactant.

Table 4. Life Cycle Inventory of the Considered Scenarios for the Syngas Production

		unit	scenario A	scenario B	scenario C	scenario D
input	natural gas	N m <sup>3</sup> /h	$3.4 \times 10^{-1}$		$2.5 \times 10^{-1}$	
	biogas	N m <sup>3</sup> /h		$7.0 \times 10^{-1}$	$4.9 \times 10^{-1}$	$4.9 \times 10^{-1}$
	biogas (fuel)	N m <sup>3</sup> /h				$6.0 \times 10^{-1}$
	water	kg/h	$3.4 \times 10^{-2}$	$7.0 \times 10^{-1}$	$5.0 \times 10^{-1}$	$5.0 \times 10^{-1}$
	oxygen	kg/h	$2.8 \times 10^{-1}$	$3.3 \times 10^{-1}$		
	air	kg/h			3.1	3.7
	P-100 <sup>a</sup>	kJ/h	$1.1 \times 10^{-1}$	2.2	1.9	1.9
	Q-100 <sup>a</sup>	kJ/h	$2.3 \times 10^2$	$4.7 \times 10^2$		
	Q-101 <sup>a</sup>	kJ/h	$1.5 \times 10^2$	$1.7 \times 10^2$		
	PVSA <sup>a</sup>	kJ/h		$5.7 \times 10^2$	$2.5 \times 10^2$	$2.5 \times 10^2$
output	syngas	N m <sup>3</sup> /h	1.0	1.0	1.0	1.0
	water	m <sup>3</sup> /h	$3.7 \times 10^{-5}$	$7.2 \times 10^{-4}$	$3.4 \times 10^{-4}$	$3.4 \times 10^{-4}$
	CO <sub>2</sub> (balance)	kg/h	$3.5 \times 10^{-2}$	$6.5 \times 10^{-2}$		
	CO <sub>2</sub> (off-gas, fossil)	kg/h			$5.0 \times 10^{-1}$	
	CO <sub>2</sub> (off-gas, biogenic)	kg/h				1.2
	CO <sub>2</sub> (PVSA)	kg/h		$7.1 \times 10^{-1}$	$3.1 \times 10^{-1}$	$3.1 \times 10^{-1}$
avoided	CO <sub>2</sub> (balance)	kg/h			$1.6 \times 10^{-1}$	$1.6 \times 10^{-1}$
	Q-102 <sup>a</sup>	kJ/h	$2.7 \times 10^2$	$2.4 \times 10^2$		
	Q-103 <sup>b</sup>	kJ/h	$3.9 \times 10^2$	$8.6 \times 10^2$		
	K-102 <sup>a</sup>	kJ/h			$3.0 \times 10^2$	$3.0 \times 10^2$
	Q-104 <sup>b</sup>	kJ/h			$2.2 \times 10^3$	$3.1 \times 10^3$
	V-100 <sup>b</sup>	kJ/h			$8.9 \times 10^2$	$8.9 \times 10^2$

<sup>a</sup>Electricity. <sup>b</sup>Heat.

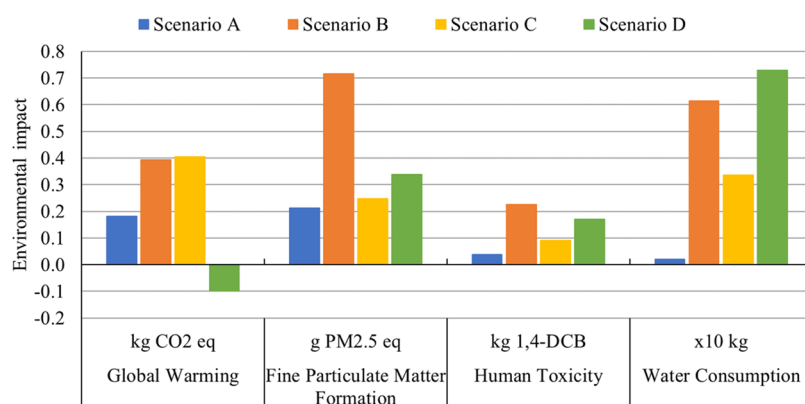


Figure 8. Environmental impact results for the different syngas production scenarios expressed as equivalent masses formed or consumed in each category (ReCiPe 2016 Midpoint H/H).

**3.3. LCA Results.** From the results obtained, the environmental impact assessment of the four different scenarios was carried out normalizing the raw data by setting the production of 1 N m<sup>3</sup> of syngas as the FU, with which the biogas-to-syngas paths were compared. The detailed LCI of each of the four scenarios is reported in Table 4.

Of the 18 impact categories that the ReCiPe method has, four were chosen as the most representative for this study: global warming (GW), fine particulate matter formation (FPMF), human toxicity (HT), and water consumption (WC). The choice fell on these categories because they showed the highest single scores (a system of the ReCiPe method to compare the impacts of different categories). The results of the analysis at the midpoint level are presented in Figure 8 and fully listed in Table S1 in the Supporting Information file.

What immediately emerged was the result of scenario D in the GW category, which showed a negative impact of  $-0.10$  kg CO<sub>2</sub> equiv. It means that when the heat demand in the S/DR process was covered by the use of CB, the whole scenario had less CO<sub>2</sub> in

the output than it was in input. This was possible thanks to the exploitation of the CO<sub>2</sub> present in the feed, which from an undesired product (as in the case of CB combustion) became a useful resource to obtain syngas. This aspect was one of the strengths of the combined S/DR process and was particularly highlighted by scenario D because the off-gases for the heating system came from a biogenic resource (CB) and their environmental impact was zero. Scenario C, despite using the same process technology as scenario D, had an impact on the GW category estimated at 0.40 kg CO<sub>2</sub> equiv because the benefit of the process was canceled by the emissions of the heating system. In fact, heating energy was obtained by the combustion of natural gas and its emissions were considered to be environmentally impacting because they derive from a fossil resource. ATR processes showed quite different impacts on GW depending on whether the feed was natural gas (scenario A) or CB (scenario B). In particular, scenario A had an impact in this category that was about half of that of scenario B, 0.18 and 0.39 kg CO<sub>2</sub> equiv, respectively. Since ATR technology is

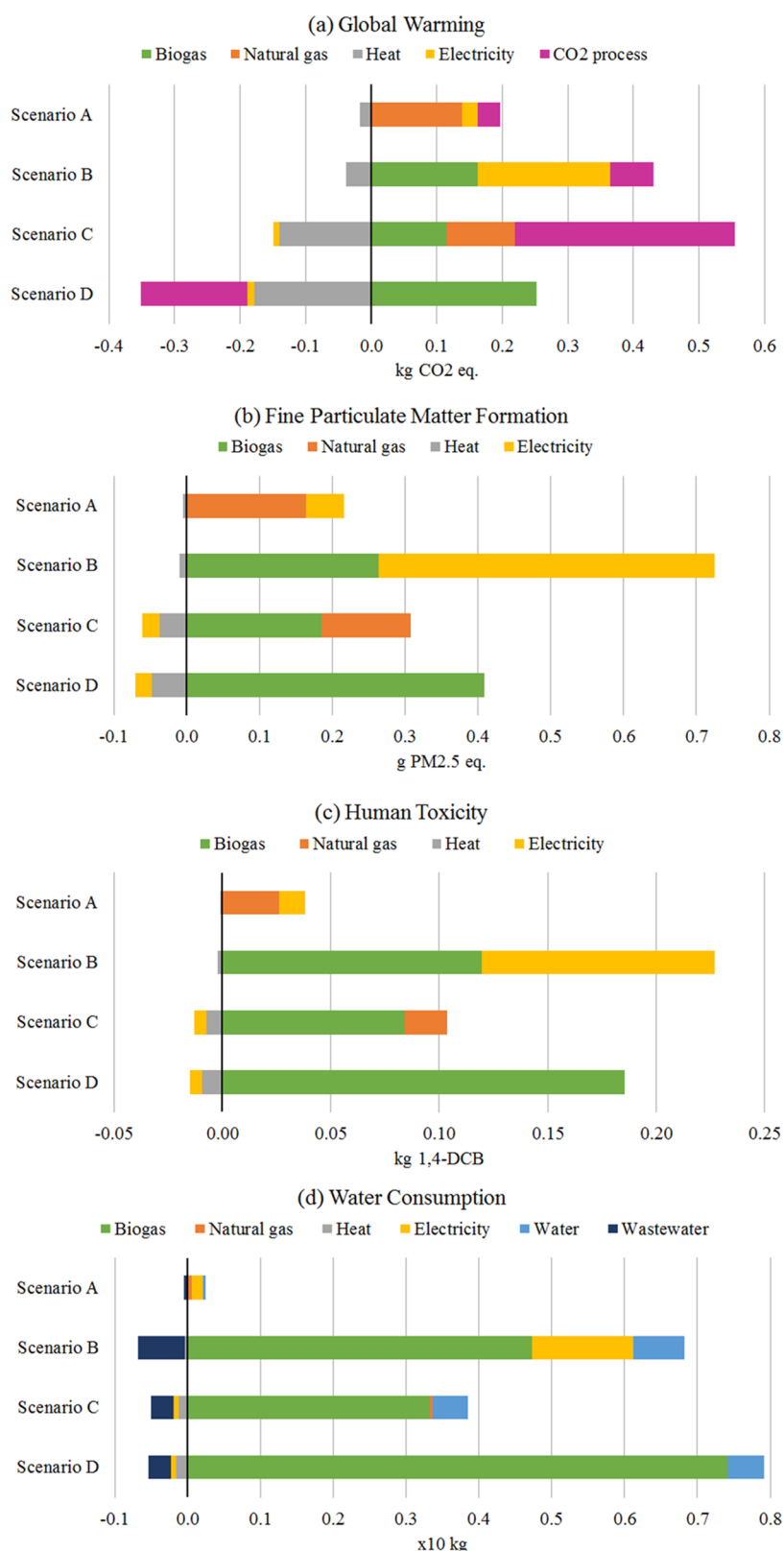


**Figure 9.** Contribution analysis for the different scenarios in (a) global warming, (b) fine particulate matter formation, (c) human toxicity, and (d) water consumption (ReCiPe 2016 Midpoint H/H).

autothermal (i.e., it does not require external heating), there were no other greenhouse gas emissions than the output residues; therefore, the reasons for this difference in impact should be investigated through a contribution analysis.

In the FPMF category, scenario B has estimated an impact of 0.72 g  $PM_{2.5}$  equiv, much greater than the others, which were between 0.21 and 0.34 g  $PM_{2.5}$  equiv. There was a higher difference between the two scenarios of the ATR process than

**Table 5. Results of Endpoint Analysis of Syngas Production Processes (ReCiPe 2016 Endpoint H/H)**

damage category	unit	scenario A	scenario B	scenario C	scenario D
human health	DALYs	$3.2 \times 10^{-7}$	$9.2 \times 10^{-7}$	$5.8 \times 10^{-7}$	$2.1 \times 10^{-7}$
ecosystems	species-year	$6.9 \times 10^{-10}$	$1.9 \times 10^{-9}$	$1.5 \times 10^{-9}$	$3.7 \times 10^{-10}$
resources	USD	$1.1 \times 10^{-1}$	$1.4 \times 10^{-2}$	$7.4 \times 10^{-2}$	$-9.0 \times 10^{-3}$

between those of the combined S/DR process, indicating that the current technology was more sensitive to the impacts of this category when switching from natural gas to CB. On the other hand, the impacts of the scenarios C and D meant that CB production implied a higher particulate formation than natural gas since the simulation of combustion off-gas did not include this type of emission.

In the HT and WC categories, processes using CB showed the highest impacts, suggesting that the cause of these results could be the CB itself. This was particularly evident in the WC category, where scenario A had an impact of one order of magnitude lower than the others (0.2 kg). The combined S/DR process used a higher S/CH<sub>4</sub> ratio than in the ATR process, but this did not affect the impacts of the category because scenario B had a comparable water consumption (6.1 kg) to scenarios C and D. These latter two scenarios seemed to confirm the CB hypothesis, because when it was used in double quantities (scenario D), the impact on water consumption also doubles (3.4 vs 7.3 kg). The same trend can also be identified in the HT category, where scenario A had half of the impact of scenario C (0.04 vs 0.09 kg 1,4-dichlorobenzene (1,4-DCB)) and scenarios B and D were the ones with the highest impacts using most CBs (see LCI in Table 4).

For a more detailed analysis of the impacts and to fully understand who was responsible for them, a contribution analysis was carried out, whose results are shown in Figure 9 and reported in Table S2 in the Supporting Information.

The contributions on the GW category confirmed the findings of the previous analysis, i.e., the combined S/DR process exploited the CO<sub>2</sub> of the feed, effectively removing it from the environment. This was highlighted in scenario D, where the "CO<sub>2</sub> process" bar depended only on the difference between the input and the output and was negative. As mentioned above, scenario C also considered the off-gases of natural gas combustion in the CO<sub>2</sub> balance and this shifted the bar to positive values. CB, however, was not free from impacts on the GW category, but, on the contrary, it had an environmental burden due to the anaerobic digestion process of organic waste. With the same volume, its impact was lower than that of natural gas (0.23 vs 0.41 kg CO<sub>2</sub> equiv/(N m<sup>3</sup>)), but since in scenario C the amount of CB was greater, the two contributions were almost equal.

Scenario B, for all of the categories, had a large impact due to electricity that compromises its environmental performance. The reason behind this great need for electricity lies in the composition of the ATR reactor output. When the feed was CB, in fact, the impurities of CO<sub>2</sub> in the output remained large, and to obtain the same quality of syngas (purity >92%, see FU), a large use of electricity was required for the PVSA process. For comparison, in scenario A, the CO<sub>2</sub> molar fraction in the output flow was 0.02 (PVSA purification was not required), in scenarios C and D, it was 0.14, and in scenario B, it was 0.28. This had the greatest effect on the FPMF and HT categories, where the contribution of electricity was 64 and 48%, respectively (scenario B). Without this contribution, the results of scenario

B would be closer to those of scenario A, which used the same type of process.

The previously formulated hypothesis on the role of CB in the HT and WC categories was confirmed by the contribution analysis. In both impact categories, CB took the lion's share when used and was the main, if not the only one, responsible for the impacts. The environmental burdens per cubic meter of CB in these categories were much higher than those of natural gas and derived from its production chain; moreover, it was used in higher volumes, which explains its weight. In particular, a contribution analysis carried out on it (Figure S1 in the Supporting Information) showed that the electricity demand of anaerobic digestion was the main cause of the environmental burden of CB. However, the environmental efficiency of this process was not further investigated as it is not part of the scope of this work. The latest analysis carried out with the ReCiPe method is the endpoint assessment of the damage caused by the scenarios. The results are reported in Table 5 and use a different unit for each category. The damages caused to human health were estimated with disability-adjusted life years (DALYs), those on ecosystems by estimating the disappearance of species per year (species-year), while the damages to resources were calculated as a function of the rising extraction costs caused by their continuous extraction and are expressed in USD.

The analysis showed that the scenarios using the ATR process were those with the highest damage, in particular scenario B in the human health and ecosystem categories and scenario A in the resources category. An impact category can affect more than one damage category, such as GW, which influences both human health and ecosystems. These two damage categories showed similar trends in results, and scenario B had the highest value, followed by scenario C, while scenarios A and D had lower values. This reflects, in general, what emerged from the analysis of the impacts on GW, FPMF, and HT categories. Scenarios B and C showed significant positive values in all three impact categories, while scenario D had a negative impact in category GW that lowers the damage to human health and ecosystems. On the other hand, the endpoint results of Table 5 showed an aspect of the processes not yet discussed, i.e., the resource consumption. Scenarios A and C clearly showed that when natural gas was used, the damage caused to the resource category was significantly affected. Scenario D showed an avoided damage to resources due to the low contribution of CB in this category and to the heat recovery that can be carried out after the S/DR reactor, while scenario B was still positive due to the high amount of electricity required.

To deepen the issue of resources, the scenarios were also analyzed using the CED method. As stated above, the CED method does not consider the negative effect (impacts or damages) of processes on the environment but provides an indicator of the intensity of resource use. Results, listed in Table 6, are expressed in energy terms and divided between nonrenewable and renewable resources.

The highest consumption was related to nonrenewable resources, even for scenarios using only biogas (B and D). This was mainly due to the electricity needs that were met by the

**Table 6. Assessment of Resource Consumption for Each Scenario Determined Using the CED Method**

process	unit	total	nonrenewable	renewable
scenario A	MJ equiv	14.69	14.64	0.04
scenario B	MJ equiv	5.97	5.31	0.67
scenario C	MJ equiv	10.92	10.65	0.27
scenario D	MJ equiv	2.28	1.68	0.59

grid and that currently involved the exploitation of fossil resources. In scenarios A and C, natural gas used in processes was directly responsible for fossil resource consumption, covering almost the entire demand of the scenarios (>97%) and responsible for the significantly higher values. The results indicated that scenario A had the greatest need for resources, while scenario D was assigned the lowest, in the middle, scenarios C and B were in the same order as they appeared in the damage analysis in the resources category of the ReCiPe method.

Further information extracted from the results on resource consumption is the renewability grade<sup>53</sup> of the scenarios (Figure 10).

It evaluates the percentage of renewable resources out of the total and shows that scenario D reaches the highest value (26%). The use of fossil resources was therefore balanced by more than 1/4 of the renewable resources, and this represents a very good step in the transition between nonrenewable technologies to renewable ones. The other process with a similar index is the scenario B (11%), and this indicates that the way to achieve the most renewable processes possible is to replace natural gas with CB. Scenarios A and C had the worst renewability rates (3 and 0.3%, respectively) and if we add to this the fact that these were also the scenarios where the demand for resources was the highest, the picture is certainly not favorable from an environmental point of view.

#### 4. CONCLUSIONS

This work was designed to evaluate the environmental performance of a model clean biogas (CB) upgrading process that combines the well-known reactions of steam and dry reforming to obtain syngas (S/DR process). To do this, the LCA methodology was applied and the current syngas production system (ATR process) was included in the study as a benchmark. The combined S/DR process used CB as the raw material, and the heat requirement can be covered by natural gas (scenario C) or by CB itself (scenario D); therefore, the ATR process has also been evaluated with both natural gas (scenario A) or CB (scenario B) feed. The consideration of all of these scenarios allowed conducting the evaluation with a from-cradle-to-gate perspective and the double feeding of the ATR process assures consistency and uniformity to the analysis.

The analysis showed that biogas-to-syngas technology using reforming processes has the potential to reduce the anthropogenic impact on the environment. According to the ReCiPe method, the combined S/DR process has proven to be comparable with the already existing and widespread industrial applications, showing similar impacts in the most representative categories of the comparison. In particular, a contribution analysis showed that the lower electricity demand (−34 and −80% compared to scenario A and scenario B, respectively) and the higher heat recovery (3–8 times higher) that the S/DR process can provide compared to ATR are driving factors in the environmental assessment of the new process and lower its impact. Furthermore, if the combined S/DR process is conducted using CB also as a heat source, the CO<sub>2</sub> balance turns negative (−0.10 kg CO<sub>2</sub>/m<sup>3</sup> of produced syngas), ensuring that the whole process has excellent potential as carbon capture and utilization (CCU) technology. This translates into the lowest weight on damage categories and can also lead to an estimated  $-9.0 \times 10^{-3}$  USD/m<sup>3</sup> avoided damage to the resource category. On the other hand, switching the inlet feed of the current ATR technology from natural gas to CB is not environmentally convenient, as the impacts are more than doubled in each category. The reasons for this behavior derive from the production chain of CB, whose contribution is accentuated in the human toxicity and water consumption categories, and from the purification step of the produced syngas, which is contaminated by input CO<sub>2</sub> when the CB is used. The latter issue is not particularly relevant for the combined S/DR process because its main characteristic is to exploit the CO<sub>2</sub> of feed as a resource rather than a waste and, therefore, the quantity to be removed downstream is half (CO<sub>2</sub> molar fraction: 0.14 vs 0.28). Therefore, although the current ATR technology has proven to be still competent and with low environmental impacts, it is strongly linked to the use of fossil fuels. When CB is used, the environmental impacts of ATR increase significantly, whereas the S/DR process has shown a higher adaptability, which is crucial for the transition to renewable resources.

Finally, the analysis of resource consumption with the cumulative energy demand (CED) method has highlighted the great weight that the use of natural gas has in this evaluation, where processes using natural gas have impacts between 2.5 and 5 times greater than their CB counterparts. It also emerged that the use of CB makes it possible to increase the renewability grade of the investigated scenarios, which increases from 0.3 to 11% in the case of the ATR technology and from 3 to 26% for the S/DR process.

To conclude, this work is part of the AES evaluations and shows that the combined S/DR process is a promising technology for the production of syngas because it can rely on CO<sub>2</sub> sequestration. Its development should therefore be encouraged and pursued, and the same should be done for

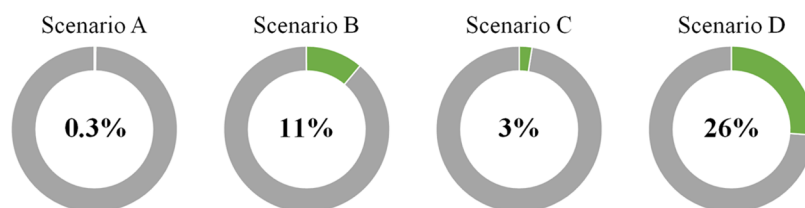


**Figure 10.** Renewability grade calculated as a percentage of renewable resources (in green) on the total (in gray) of each route determined using the CED method.

biogas production, which has shown some environmental weakness. Its improvement would make it possible to further reduce the environmental burden of the overall process, which is essential to achieve sustainable development.

## ■ ASSOCIATED CONTENT

### Supporting Information

The Supporting Information is available free of charge at <https://pubs.acs.org/doi/10.1021/acs.energyfuels.0c04066>.

Impact assessment of the scenarios in terms of ReCiPe 2016 Midpoint H/H (Table S1); contribution analysis of scenarios in the four considered impact categories (Table S2); contribution analysis in biogas production (Figure S1) (PDF)

Simulation results and respective material stream and compositions (ZIP)

## ■ AUTHOR INFORMATION

### Corresponding Authors

Nicola Schiaroli – Dipartimento di Chimica Industriale “Toso Montanari”, 40136 Bologna, Italy; Email: [nicola.schiaroli@unibo.it](mailto:nicola.schiaroli@unibo.it)

Mirco Volanti – Dipartimento di Chimica Industriale “Toso Montanari”, 40136 Bologna, Italy; Email: [mirco.volanti@unibo.it](mailto:mirco.volanti@unibo.it)

Carlo Lucarelli – Dipartimento di Scienza e Alta Tecnologia, 22100 Como, Italy; [orcid.org/0000-0002-5098-0575](https://orcid.org/0000-0002-5098-0575); Email: [carlo.lucarelli@uninsubria.it](mailto:carlo.lucarelli@uninsubria.it)

### Authors

Antonio Crimaldi – Dipartimento di Chimica Industriale “Toso Montanari”, 40136 Bologna, Italy

Fabrizio Passarini – Dipartimento di Chimica Industriale “Toso Montanari”, 40136 Bologna, Italy; [orcid.org/0000-0002-9870-9258](https://orcid.org/0000-0002-9870-9258)

Angelo Vaccari – Dipartimento di Chimica Industriale “Toso Montanari”, 40136 Bologna, Italy

Giuseppe Fornasari – Dipartimento di Chimica Industriale “Toso Montanari”, 40136 Bologna, Italy

Sabrina Copelli – Dipartimento di Scienza e Alta Tecnologia, 22100 Como, Italy; [orcid.org/0000-0001-6070-3718](https://orcid.org/0000-0001-6070-3718)

Federico Florit – Dipartimento di Chimica ed Ingegneria Chimica “G. Natta”, 20131 Milano, Italy; [orcid.org/0000-0002-6484-4953](https://orcid.org/0000-0002-6484-4953)

Complete contact information is available at:

<https://pubs.acs.org/doi/10.1021/acs.energyfuels.0c04066>

### Author Contributions

This manuscript was written through contributions of all authors. All authors have given approval to the final version of the manuscript.

### Notes

The authors declare no competing financial interest.

## ■ ABBREVIATIONS

S/DR = steam dry reforming

CB = clean biogas

BM = biomethane

LCA = life cycle assessment

ATR = autothermal reforming

CCU = carbon capture and utilization

GHG = greenhouse gasses

DR = dry reforming

GHSV = gas hourly space velocity

PVSA = pressure vacuum swing adsorption

LCI = life cycle inventory

FU = functional unit

CED = cumulative energy demand

GW = global warming

FPMF = fine particulate matter formation

HT = human toxicity

WC = water consumption

## ■ REFERENCES

- (1) Nevzorova, T.; Kutcherov, V. Barriers to the wider implementation of biogas as a source of energy; A state-of-the-art review. *Energy Strategy Rev.* **2019**, *26*, No. 100414.
- (2) Weiland, P. Biogas production: current state and perspectives. *Appl. Microbiol. Biotechnol.* **2010**, *85*, 849–860.
- (3) Angelidaki, I.; Treu, L.; Tsapekos, P.; Luo, G.; Campanaro, S.; Wenzel, H.; Kougias, P. G. Biogas upgrading and utilization: current status and perspectives. *Biotechnol. Adv.* **2018**, *36*, 452–466.
- (4) Khan, I. U.; Othman, M. H. D.; Hashim, H.; Matsuura, T.; Ismail, A. F.; Arzhandi, M. R. D.; Azelee, I. W. Biogas as a renewable energy fuel – A review of biogas upgrading, utilisation and storage. *Energy Convers. Manage.* **2017**, *150*, 277–294.
- (5) Andriani, D.; Wresta, A.; et al. A review on optimization production and upgrading biogas through CO<sub>2</sub> removal using various techniques. *Appl. Biochem. Biotechnol.* **2014**, *172*, 1909–1928.
- (6) Scarlat, N.; Dallemand, J. F.; Fahl, F. Biogas: developments and perspectives in Europe. *Renewable Energy* **2018**, *129*, 457–472.
- (7) Lange, J.-P. Methanol synthesis: a short review of technology improvements. *Catal. Today* **2001**, *64*, 3–8.
- (8) Van Bennekom, J. G.; Venderbosch, R. H.; Winkelman, J. G. M.; Wilbers, E.; Assink, D.; Lemmens, K. P. J.; Heeres, H. J. Methanol synthesis beyond chemical equilibrium. *Chem. Eng. Sci.* **2013**, *87*, 204–208.
- (9) Montebelli, A.; Visconti, C. G.; Groppi, G.; Tronconi, E.; Kohler, S. Optimization of compact multitubular fixed-bed reactors for the methanol synthesis loaded with highly conductive structured catalysts. *Chem. Eng. J.* **2014**, *255*, 257–265.
- (10) Aasberg-Petersen, K.; Dybkjær, I.; Ovesen, C. V.; Schjødt, N. C.; Sehested, J.; Thomsen, S. G. Natural gas to synthesis gas – Catalysts and catalytic processes. *J. Nat. Gas. Sci. Eng.* **2011**, *3*, 423–459.
- (11) Shi, C.; Elgarni, M.; Mahinpey, N. Process design and simulation study: CO<sub>2</sub> utilization through mixed reforming of methane for methanol synthesis. *Chem. Eng. Sci.* **2021**, *233*, No. 116364.
- (12) Maqbool, W.; Lee, E. S. Syngas production process development and economic evaluation for Gas-To-Liquid applications. *Chem. Eng. Technol.* **2014**, *37*, 995–1001.
- (13) Perregaard, J. Methanol synthesis at near-critical conditions combined with ATR synthesis gas technology. The technology choice for large-scale methanol production. *Catal. Today* **2005**, *106*, 99–102.
- (14) Dahl, P. J.; Christensen, T. S.; Winter-Madsen, S.; King, S. M. In *Proven Autothermal Reforming Technology for Modern Large-Scale Methanol Plants, Nitrogen + Syngas*, International Conference and Exhibition, 2014.
- (15) Rostrup-Nielsen, J. R.; Sehested, J.; Nørskov, J. K. Hydrogen and synthesis gas by steam- and CO<sub>2</sub> reforming. *Adv. Catal.* **2002**, *47*, 65–139.
- (16) Meloni, E.; Martino, M.; Palma, V. A short review of Ni based catalysts and related engineering issues for methane steam reforming. *Catalysts* **2020**, *10*, 352–389.
- (17) Quirino, P. P. S.; Amaral, A.; Pontes, K. V.; Rossi, F.; Manenti, F. Modeling and Simulation of an Industrial Top-Fired Methane Steam Reforming Unit. *Ind. Eng. Chem. Res.* **2020**, *59*, 11250–11264.
- (18) Yang, L.; Ge, X.; Wan, C.; Yu, F.; Yebo, L. Progress and perspectives in converting biogas to transportation fuels. *Renewable Sustainable Energy Rev.* **2014**, *40*, 1133–1152.

- (19) Kumar, N.; Shojae, M.; Spivey, J. J. Catalytic bi-reforming of methane: from greenhouse gases to syngas. *Curr. Opin. Chem. Eng.* **2015**, *9*, 8–15.
- (20) Olah, G. A.; Goepfert, A.; Czaun, M.; Surya Prakash, G. K. Bi-reforming of methane from any source with steam and carbon dioxide exclusively to metgas (CO-2H<sub>2</sub>) for methanol and hydrocarbon synthesis. *J. Am. Chem. Soc.* **2013**, *135*, 648–650.
- (21) Jabbour, K. Tuning combined steam and dry reforming of methane for “metgas” production: A thermodynamic approach and state-of-the-art catalysts. *J. Energy Chem.* **2020**, *48*, 54–91.
- (22) Schiaroli, N.; Lucarelli, C.; Sanghez de Luna, G.; Fornasari, G.; Vaccari, A. Ni-based catalysts to produce synthesis gas by combined reforming of clean biogas. *Appl. Catal., A* **2019**, *582*, No. 117087.
- (23) Kumar, N.; Shojae, M.; Spivey, J. J. Catalytic bi-reforming of methane: from greenhouse gases to syngas. *Curr. Opin. Chem. Eng.* **2015**, *9*, 8–15.
- (24) Jang, W.-J.; Shim, J.-O.; Kim, H.-M.; Yoo, S.-Y.; Roh, H.-S. A review on dry reforming of methane in aspect of catalytic properties. *Catal. Today* **2019**, *324*, 15–26.
- (25) Hakawati, R.; Smyth, B. M.; McCullough, G.; De Rosa, F.; Rooney, D. What is the most energy efficient route for biogas utilization: Heat, electricity or transport? *Appl. Energy* **2017**, *206*, 1076–1087.
- (26) Hajjaji, N.; Martinez, S.; Trably, E.; Steyer, J. P.; Helias, A. Life cycle assessment of hydrogen production from biogas reforming. *Int. J. Hydrogen Energy* **2016**, *41*, 6064–6075.
- (27) Battista, F.; Montenegro Camacho, Y. S.; Hernández, S.; Bensaid, S.; Herrmann, A.; Krause, H.; Trimis, D.; Fino, D. LCA evaluation for the hydrogen production from biogas through the innovative BioRobur project concept. *Int. J. Hydrogen Energy* **2017**, *42*, 14030–14043.
- (28) Di Marcoberardino, G.; Liao, X.; Dauriat, A.; Binotti, M.; Manzolini, G. Life Cycle Assessment and Economic Analysis of an Innovative Biogas Membrane Reformer for Hydrogen Production. *Processes* **2019**, *7*, 86–99.
- (29) Navas-Anguita, Z.; Cruz, P. L.; Martín-Gamboa, M.; Iribarren, D.; Dufour, J. Simulation and life cycle assessment of synthetic fuels produced via biogas dry reforming and Fischer-Tropsch synthesis. *Fuel* **2019**, *235*, 1492–1500.
- (30) Nguyen, T. T. H.; Yamaki, T.; Taniguchi, S.; Endo, A.; Kataoka, S. Integrating life cycle assessment for design an optimization of methanol production from combined methane dry reforming and partial oxidation. *J. Cleaner Prod.* **2021**, No. 125970.
- (31) Chen, L.; Gangadharan, P.; Lou, H. H. Sustainability assessment of combined steam and dry reforming versus tri-reforming of methane for syngas production. *Asia-Pac. J. Chem. Eng.* **2018**, *13*, No. e2168.
- (32) <https://www.grc.nasa.gov/www/CEAWeb/>.
- (33) ISO 14040. Environmental Management—Life Cycle Assessment—Principles and Framework, 2006.
- (34) ISO 14040. Environmental Management—Life Cycle Assessment—Requirements and Guidelines, 2006.
- (35) Aresta, M.; Galatola, M. Life cycle analysis applied to the assessment of the environmental impact of alternative synthetic processes. The dimethylcarbonate case: part I. *J. Cleaner Prod.* **1999**, *7*, 181–193.
- (36) Burgess, A. A.; Brennan, D. J. Application of life cycle assessment to chemical processes. *Chem. Eng. Sci.* **2001**, *56*, 2589–2604.
- (37) Portha, J.-F.; Jaubert, J.-N.; Louret, S.; Pons, M.-N. Life Cycle Assessment Applied to Naphtha Catalytic Reforming. *Oil Gas Sci. Technol.* **2010**, *65*, 793–805.
- (38) Jacquemin, L.; Pontalier, P.-Y.; Sablayrolles, C. Life cycle assessment (LCA) applied to the process industry: a review. *Int. J. Life Cycle Assess.* **2012**, *17*, 1028–1041.
- (39) Kralisch, D.; Ott, D.; Gericke, D. Rules and benefits of Life Cycle Assessment in green chemical process and synthesis design: a tutorial review. *Green Chem.* **2015**, *17*, 123–145.
- (40) Parvatker, A. G.; Eckelman, M. J. Comparative Evaluation of Chemical Life Cycle Inventory Generation Methods and Implications for Life Cycle Assessment Results. *ACS Sustainable Chem. Eng.* **2019**, *7*, 350–367.
- (41) Kleinekorte, J.; Fleitmann, L.; Bachmann, M.; Kätelhön, A.; Barbosa-Póvoa, A.; von der Assen, N.; Bardow, A. Life Cycle Assessment for the Design of Chemical Processes, Products, and Supply Chains. *Annu. Rev. Chem. Biomol. Eng.* **2020**, *11*, 203–233.
- (42) Patel, A. D.; Meesters, K.; Den Uil, H.; De Jong, E.; Blok, K.; Patel, M. K. Sustainability assessment of novel chemical processes at early stage: application to biobased processes. *Energy Environ. Sci.* **2012**, *5*, 8430–8444.
- (43) Patel, A. D.; Meesters, K.; Den Uil, H.; De Jong, E.; Worrell, E.; Patel, M. K. Early-Stage Comparative Sustainability Assessment of New Bio-based Processes. *ChemSusChem* **2013**, *6*, 1724–1736.
- (44) Hetherington, A. C.; Borrión, A. L.; Griffiths, O. G.; McManus, M. C. Use of LCA as a development tool within early research: Challenges and issues across different sectors. *Int. J. Life Cycle Assess.* **2014**, *19*, 130–143.
- (45) Cespi, D.; Cucciniello, R.; Ricciardi, M.; Capacchione, C.; Vassura, I.; Passarini, F.; Proto, A. A simplified early stage assessment of process intensification: glycidol as a value-added product from epichlorohydrin industry wastes. *Green Chem.* **2016**, *18*, 4559–4570.
- (46) *SimaPro Software*, version 9.1; PRé Consultants BV, 2020.
- (47) Wernet, G.; Bauer, C.; Steubing, B.; Reinhard, J.; Moreno-Ruiz, E.; Weidema, B. The Ecoinvent Database Version 3 (Part I): Overview and Methodology. *Int. J. Life Cycle Assess.* **2016**, *21*, 1218–1230.
- (48) Neri, E.; Passarini, F.; Cespi, D.; Zoffoli, F.; Vassura, I. Sustainability of a bio-waste treatment plant: Impact evolution resulting from technological improvements. *J. Cleaner Prod.* **2018**, *171*, 1006–1019.
- (49) Domènech, X.; Ayllón, J. A.; Peral, J.; Rieradevall. How Green Is a Chemical Reaction? Application of LCA to Green Chemistry. *Environ. Sci. Technol.* **2002**, *36*, 5517–5520.
- (50) Volanti, M.; Cespi, D.; Passarini, F.; Neri, E.; Cavani, F.; Mizsey, P.; Fozer, D. Terephthalic acid from renewable sources: early-stage sustainability analysis of a bio-PET precursor. *Green Chem.* **2019**, *21*, 885–896.
- (51) Huijbregts, M. A. J.; Steinmann, Z. J. N.; Elshout, P. M. F.; Stam, G.; Veronesi, F.; Vieira, M. D. M.; Hollander, A.; Zijp, M.; van Zelm, R. *ReCiPe 2016—A Harmonized Life Cycle Impact Assessment Method at Midpoint and Endpoint Level*; National Institute for Public Health and the Environment (RIVM), 2020. <https://www.rivm.nl/bibliotheek/rapporten/2016-0104.pdf> (accessed Oct, 2020).
- (52) Frischknecht, R.; Jungbluth, N. *Implementation of Life Cycle Impact Assessment Methods*; Swiss Centre for Life Cycle Inventories, 2007.
- (53) Tripodi, A.; Bahadori, E.; Cespi, D.; Passarini, F.; Cavani, F.; Tabanelli, T.; Rossetti, I. Acetonitrile from Bioethanol Ammoxidation: Process Design from the Grass-Roots and Life Cycle Analysis. *ACS Sustainable Chem. Eng.* **2018**, *6*, 5441–5451.